

# Multi-view Passive 3D Reconstruction : Comparison and Evaluation of Three Techniques and A New Method for 3D Object Reconstruction

Soulaiman El hazzat<sup>(1)</sup>, Abderrahim Saaidi<sup>(1,2)</sup>, Khalid Satori<sup>(1)</sup>

<sup>(1)</sup>LIIAN, Department Of Mathematics and informatics, Faculty of Sciences Dhar- Mahraz,  
 Sidi Mohamed Ben Abdellah University, Fes, Morocco

<sup>(2)</sup>LIMAO, Department of Mathematics, physics and informatics, polydisciplinary Faculty of Taza,  
 Sidi Mohamed Ben Abdellah University, Taza, Morocco

E-mail : soulaiman.elhazzat@yahoo.fr, Saaidi.abde@yahoo.fr, khalidsatorim3i@yahoo.fr

**Abstract—** In this article, we focus on the comparison of the passive techniques of multi-view 3D reconstruction, namely the following techniques : Passive Stereo vision, Shape from Silhouette and Space Carving. Available data in the Passive techniques are no more than one or many images taken from different point of views (using one or several cameras). These images will be used in order to render the three-dimensional scene. Our study is based on the quality of the solution (3D Model obtained) and the calculation time. In passive stereo vision, the quality of the results is evaluated in terms of the value of the re-projection error. Also we will evaluate each technique separately. In the end, to enjoy the benefits of the techniques studied we proposed a method based on the extraction of silhouette images and the matching between images to make full 3D object reconstruction. The results of our own implementation of the different techniques studied and the proposed method enable to compare and evaluate these techniques, and to show the quality of the results obtained by the proposed method.

**Keywords-**3D reconstruction; passive stereo vision; shape from silhouette; space carving.

## I. INTRODUCTION

The 3D reconstruction from images is an important and very active subject in computer vision, it has many applications: robotics, surveillance, measurement, automatic reconstruction of virtual environments, aerial reconnaissance, etc.

Many techniques suggest solutions to this problem. In this paper we are interested in Passive techniques of 3D reconstruction from multiple images, and exactly the comparison between Passive Stereo vision, Shape from Silhouette and Space Carving.

All these techniques require calibration or self-calibration of cameras used, that is to say estimating the parameters of cameras. For our study, we choose to use a 3D pattern to calibrate the cameras. There are several other methods for calibration [1] or self-calibration [2, 3] of the cameras.

Passive Stereo vision [6, 7, 8, 9] is based on the matching between different images. The matching may be dense, quasi-dense or sparse. This technique begins with the extraction of a set of points of interest that are easy to be matched. The Harris detector [4], the Sift method [5] may be used in the extraction of the points of interest. Sift descriptors [5] or ZNCC method and other techniques are used in the matching of these points. The position of a 3D point in the scene can be recovered from these matches and parameters of the cameras estimated during the calibration or self-calibration by optical triangulation.

The volumetric approaches: Shape from Silhouette [12, 15], Space Carving [16, 17] are based on a discretization of space into basic elements called voxels (figure 1(a)), the quality of the results obtained depend on the chosen resolution (number of voxels). Shape from Silhouette approach is based on the intersection of the silhouette cones associated with all image silhouettes and defines an approximate geometry of the object called the Visual Hull. Space carving approach is to assess the consistency of each voxel. In this approach, an octree representation [17] can be used (figure 1(b)), the octree structure is a tree in which each node has eight children, who become parents in their turn. This is repeated until the desired resolution is gained. Using the octree enables a faster reconstruction of the 3D model.

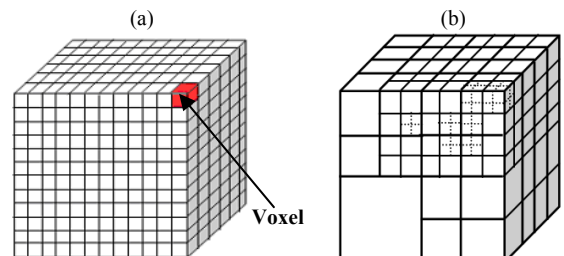


Figure 1. (a) Voxel grid (b) Octree representation

The process of reconstruction for each technique will be detailed in the following paragraphs.

This article is organized in this way : section II presents the model and the camera calibration. Section III is devoted to the description and evaluation of the technique for 3D reconstruction by Stereo vision. In section IV, Shape from Silhouette technique is presented and evaluated. In section V, the presentation and evaluation of Space Carving technique. The comparison between the different techniques of 3D reconstruction is presented in section VI. A new method of 3D object reconstruction is presented in section VII. Finally, the conclusion is presented in section VIII.

## II. CAMERA MODEL AND CALIBRATION

### A. Pinhole Camera Model

The pinhole model (Figure 2) consists of the image plane and the optical center  $O$ . A point  $M_i = (X_i, Y_i, Z_i)^T$  of the 3D scene is projected onto the image plane at a  $m_i = (u_i, v_i)^T$  point. This perspective projection is represented by the following formula :

$$\begin{pmatrix} \lambda u_i \\ \lambda v_i \\ \lambda \end{pmatrix} = \begin{pmatrix} p_{11} & p_{12} & p_{13} & p_{14} \\ p_{21} & p_{22} & p_{23} & p_{24} \\ p_{31} & p_{32} & p_{33} & p_{34} \end{pmatrix} \begin{pmatrix} X_i \\ Y_i \\ Z_i \\ 1 \end{pmatrix} \quad (1)$$

$\lambda$  : is a factor of homogeneity

$P = (p_{ij})_{i=1 \dots 3}^{j=1 \dots 4}$  : is the perspective projection matrix

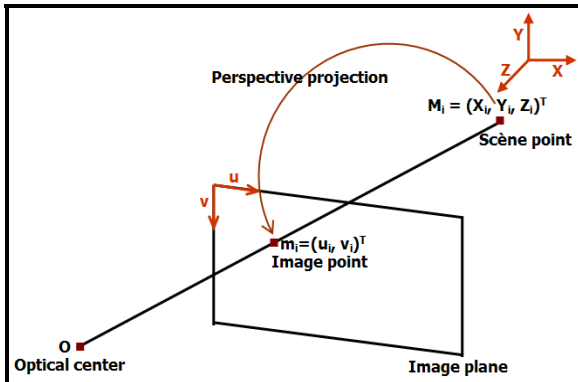


Figure 2. Pinhole camera model

### B. Calibration

The camera calibration consists in estimating the perspective projection matrix  $P$  that contains the parameters of the model. 3D Calibration Pattern (Figure 3) was used to estimate this matrix.

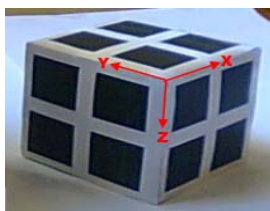


Figure 3. 3D Calibration Pattern

From equation (1), we deduce :

$$\begin{aligned} X_i p_{11} + Y_i p_{12} + Z_i p_{13} + p_{14} - u_i X_i p_{31} - u_i Y_i p_{32} - u_i Z_i p_{33} &= u_i p_{34} \\ X_i p_{21} + Y_i p_{22} + Z_i p_{23} + p_{24} - v_i X_i p_{31} - v_i Y_i p_{32} - v_i Z_i p_{33} &= v_i p_{34} \end{aligned} \quad (2)$$

Each point  $M_i$  of our 3D Calibration Pattern with known coordinates  $(X_i, Y_i, Z_i)$  is projected onto the image plane at a coordinate point  $(u_i, v_i)$ , provides the equations (2). These equations are linear over the coefficients of  $P$ . Therefore at least 6 non-coplanar points are needed to determine  $P$ .

## III. PASSIVE STEREO VISION

The simplest process of stereo vision uses only two images, it is the binocular stereo vision. Indeed, for the 3D reconstruction we need more than two images for a complete reconstruction of the object or the whole scene.

For this technique, the main difficulty comes from the problem of matching.

In this work, the matching step is performed using the ZNCC correlation measure. For a window size  $(2N+1) \times (2P+1)$ , it is defined by :

$$\text{ZNCC } (m_1(u_1, v_1), m_2(u_2, v_2)) = \frac{A}{\sqrt{B \times C}} \quad (3)$$

With :

$$\begin{aligned} A &= \sum_{i=-N}^N \sum_{j=-P}^P (I_1(u_1 + i, v_1 + j) - \overline{I_1(u_1, v_1)}) \times (I_2(u_2 + i, v_2 + j) - \overline{I_2(u_2, v_2)}) \\ B &= \sum_{i=-N}^N \sum_{j=-P}^P (I_1(u_1 + i, v_1 + j) - \overline{I_1(u_1, v_1)})^2 \\ C &= \sum_{i=-N}^N \sum_{j=-P}^P (I_2(u_2 + i, v_2 + j) - \overline{I_2(u_2, v_2)})^2 \\ \overline{I_1(u_1, v_1)} &= \frac{1}{(2N+1)(2P+1)} \sum_{i=-N}^N \sum_{j=-P}^P I_1(u_1 + i, v_1 + j) \\ \overline{I_2(u_2, v_2)} &= \frac{1}{(2N+1)(2P+1)} \sum_{i=-N}^N \sum_{j=-P}^P I_2(u_2 + i, v_2 + j) \end{aligned}$$

### A. Sparse 3D Reconstruction [9]

The reconstruction process can be described as:

- Calibration: the estimation of the parameters of cameras.
- Interest point Detection : the Harris detector [4] was used in this work.
- Interest point Matching : is to find for a point of the image 1 a correspondent in the image 2.
- Optical triangulation : it involves estimating the 3D coordinates from the matched points and the estimated projection matrices.

#### 1) Realisation

All these experiments are executed on a machine DELL Inspiron with Core 2 Duo processor 2 GHz, 2 GB of RAM memory. Different algorithms have been implemented in Java.

JAMA Library has been used for matrix computations, Jcg for the creation of 3D meshes and Java 3D API for 3D visualization.

A digital camera was used for capturing a set of images from different viewpoints. The resolution used is  $640 \times 480$  pixels.



Figure 4. Three images of the captured images

- Matching : first we began with the extraction of a set of interest points by Harris detector [4]. Then, the ZNCC method was used to make the matching of these various points.



Figure 5. Interest point matching

- The 3D points are calculated from these matches and projection matrices estimated during the calibration phase.

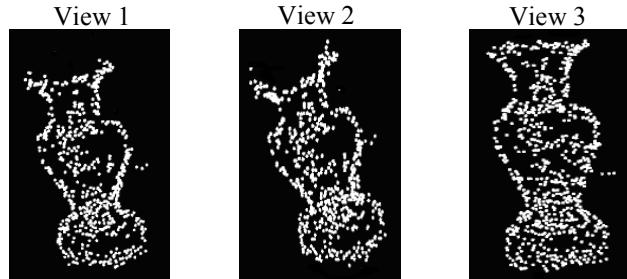


Figure 6. Reconstructed 3D points after optical triangulation  
ZNCCthreshold=0.8

TABLE I. RESULTS OF RECONSTRUCTION BASED ON THE VALUE OF THE ZNCCTHRESHOLD CHOSEN AFTER THE ELIMINATION OF THE FALSE MATCHES BY RANSAC ALGORITHM

| ZNCCthreshold value            | 0.9  | 0.85 | 0.8  | 0.75 | 0.7  | 0.6  |
|--------------------------------|------|------|------|------|------|------|
| Number of reconstructed points | 175  | 277  | 309  | 386  | 455  | 527  |
| Calculation time (in Sec.)     | 5.12 | 5.22 | 5.29 | 5.41 | 5.56 | 5.7  |
| The re-projection error        | 0.23 | 0.31 | 0.42 | 0.71 | 0.82 | 0.95 |

The result of the sparse 3D reconstruction is a sparse cloud of 3D points, to find the shape of the object and obtain a surface representation, the 3D Delaunay triangulation [20] and the 3D Crust method [20] has been used.

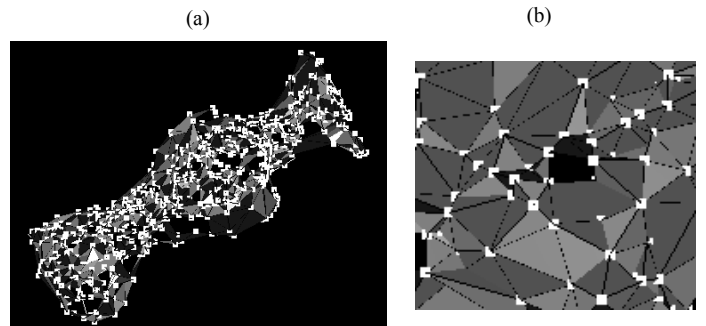


Figure 7. (a) Obtained 3D model after the application of 3D Delaunay and 3D Crust on the reconstructed points (b) Zoom on a part of the obtained 3D model

TABLE II. RESULTS OF RECONSTRUCTION AFTER THE APPLICATION OF 3D DELAUNAY TRIANGULATION AND 3D CRUST ALGORITHM ON THE RECONSTRUCTED POINTS

| ZNCCthreshold value         | 0.9 | 0.85 | 0.8 | 0.75 | 0.7  | 0.6  |
|-----------------------------|-----|------|-----|------|------|------|
| Number of calculated facets | 412 | 637  | 737 | 961  | 1090 | 1264 |
| Extra time (in Sec.)        | 3   | 5    | 7   | 9    | 11   | 14   |

## 2) Evaluation

- By reducing the value of ZNCCthreshold, the number of reconstructed points increases because we will have more matches. In the matching step, there may be some false matches. To avoid these matches as much as possible, the RANSAC algorithm [18] was used. This algorithm is based on the epipolar constraint given by the following formula :

$$m_2^T F m_1 = 0 \quad (4)$$

With  $(m_1, m_2)$  : is a pair of corresponding points.

$F$  : is the fundamental matrix (3x3 matrix)

- Having reliable matches and a reliable estimation of the projection matrices allow a good quality reconstruction. According to the results presented in Table 1, the value of the reprojection error defined by (5) shows the quality of the different results

$$Err = \frac{1}{2n} \sum_{i=1}^n (d(P_1 M_i, m_{1i})^2 + d(P_2 M_i, m_{2i})^2) \quad (5)$$

$n$  : The number of matches (number of 3D points).

$P_1$  and  $P_2$ : projection matrices

$(m_{1i}, m_{2i})$ : is a pair of corresponding points.

$M_i$  : reconstructed 3D point from  $(m_{1i}, m_{2i})$ .

### B. Quasi-Dense 3D reconstruction [10, 22]

The propagation method [10, 11] receives as input a set of initial matches (germs). The treatment consists in looking for new matches in the vicinity of the old ones, the couples of points whose correlation score (ZNCC) is above a threshold that verify the epipolar constraint are kept.

#### 1) Realisation :

After the application of the propagation method [10, 11] on 175 initial matches, the following results were obtained (different thresholds of ZNCC score are tested).

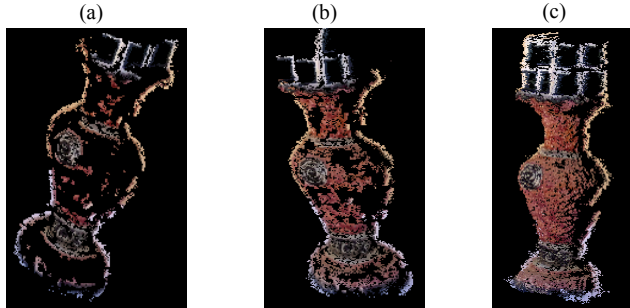


Figure 8. 3D reconstructed model after the application of the propagation method (a) ZNCCthreshold = 0.9 (b) ZNCCthreshold = 0.8 (c) ZNCCthreshold = 0.6

TABLE III. NUMBER OF RECONSTRUCTED POINTS AFTER APPLICATION OF THE PROPAGATION METHOD AS A FUNCTION OF THE VALUE OF THE ZNCCTHRESHOLD CHOSEN

| ZNCCthreshold value            | 0.9  | 0.85 | 0.8   | 0.75  | 0.7   | 0.6   |
|--------------------------------|------|------|-------|-------|-------|-------|
| Number of reconstructed points | 6620 | 8770 | 12056 | 15876 | 18765 | 21123 |
| Calculation time (in Sec.)     | 35   | 49   | 76    | 96    | 115   | 153   |
| The re-projection error        | 0.87 | 0.9  | 0.92  | 1.05  | 1.14  | 1.12  |

#### 2) Evaluation :

- With a big value of ZNCCthreshold (0.9, 0.8) the number of reconstructed points is insufficient to define the shape of the object. However, for a small value ZNCCthreshold (0.6) we obtain a number of 3D points sufficient to define the shape of the object.
- The calculation time increases with the increase in number of reconstructed 3D points.

### IV. SHAPE FROM SILHOUETTE

Shape from Silhouette [12, 15], also called the Visual Hull, is a technique which allows to reconstruct a 3D bounding shape of the objects from the observed silhouettes in each view.

The extraction of the silhouettes [13, 14] is an important part of the reconstruction process because the quality of the reconstruction result strongly depends on the quality of the silhouettes extraction from images

In this work, we are interested in the volumetric approach working on a voxel grid (approximation of the Visual Hull by a set of voxels), it consists in eliminating for each camera the voxels outside the cone of silhouette (Figure 9).

This technique is widely used for 3D shape estimation because of its simplicity and speed. But it has some disadvantages : it is not possible to reconstruct concavities of an object, and the reconstruction result is not very accurate when the number of views used is low. Other approaches [16, 17, 19, 21] propose the use of color information to estimate more precisely the form and have a textured 3D model.

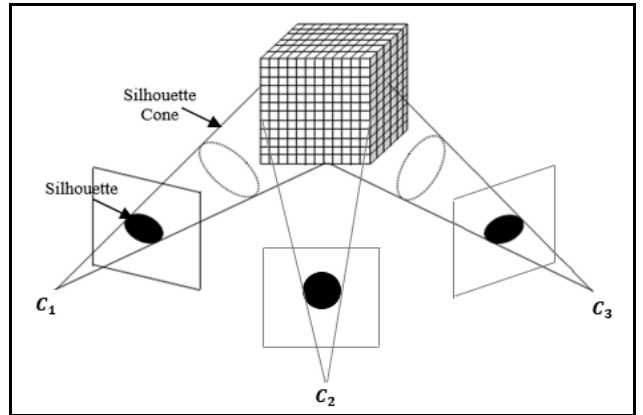


Figure 9. Principle of Shape from Silhouette technique

#### A. Realisation

First we start with the calibration of cameras, after we move to the extraction of silhouettes of different images taken from different viewpoints. This is an important part of the reconstruction process that is performed by using various approaches [13, 14]. Examples of silhouettes can be seen in figure 10.

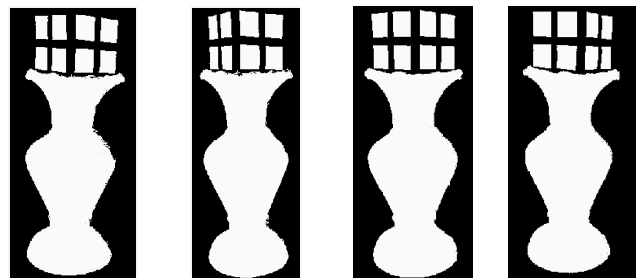


Figure 10. Silhouettes extraction after segmentation

The visual hull Reconstruction from eight images of  $640 \times 480$  pixels is presented in the figure 11.

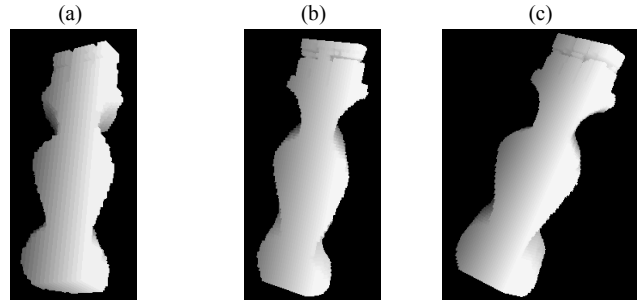


Figure 11. Reconstruction results by Shape From Silhouette technique  
(a) grid resolution : 30x30x60 (b) grid resolution : 60x60x80 (c) grid resolution : 80x80x100

TABLE IV. RESULT OF RECONSTRUCTION BY SHAPE FROM SILHOUETTE TECHNIQUE

| Resolution           | 30*30*60 | 60*60*80 | 80*80*100 |
|----------------------|----------|----------|-----------|
| Number of voxels     | 10789    | 26098    | 48185     |
| Calculation time (s) | 6        | 15       | 29        |

#### B. Evaluation :

The quality of the results obtained depends on :

- Resolution chosen : the more the resolution is great, the more the reconstructed form is of quality and close to reality, and the more likely it is to rebuild exact details.
- The number of images used : a large number of images enables a closer solution of reality. When the number of views is reduced the reconstruction is little precise.
- Silhouette extraction errors directly affect the quality of reconstruction.
- The major drawback of this approach is that all the concavities present in the silhouette images cannot be represented.

## V. SPACE CARVING

The Shape from Silhouette approach allows the approximate estimation of the shape of the object (Visual hull). The Space Carving approach [16, 17] uses the color information to estimate the shape more precisely. Moreover, it allows to have a textured model. It is an approach based on voxels. The process of reconstruction (Figure 13) begins with the initialization of a volume containing the scene (the object), Discretized in voxels (voxel grid). For each visible voxel a validation test compares the color of pixels on which this voxel is projected. If these colors are similar, this voxel is photo-consistent and it is validated as belonging to the surface of the object. The Voxels that are not photo-consistent are removed. The result of the reconstruction is the set of photo-consistent remaining voxels.

In order to ensure that all cameras are considered and have a complete reconstruction of the scene (the object). The photo-consistent voxels research must be carried out in the 6 directions of space 3D (voxel space) (Figure 12).

Space Carving approaches produce an estimation of the form more accurate than those proposed by Shape from Silhouette approaches but it requires longer calculation time.

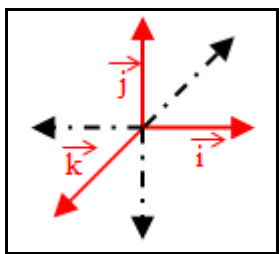


Figure 12. The 6 directions of 3D space

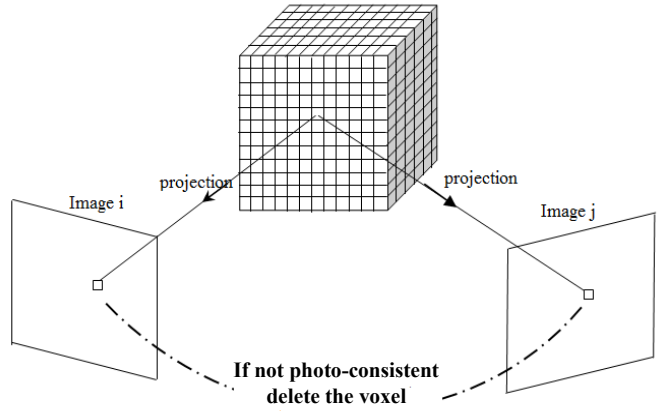


Figure 13. Principle of Space Carving technique

#### A. Realisation

First the cameras are calibrated. The same images used in the shape from silhouette technique are used here.

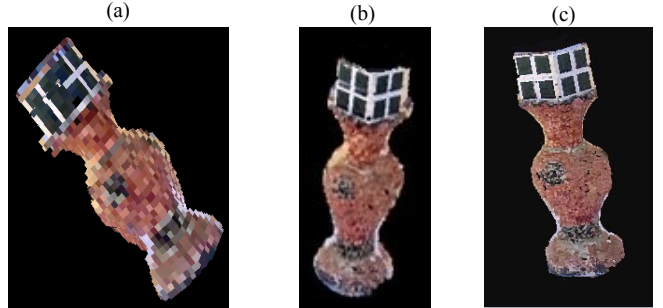


Figure 14. Results of 3D reconstruction by Space Carving technique  
(a) resolution 30x30x60 (b) resolution 60x60x80 (c) resolution 80x80x100

TABLE V. RESULT OF THE 3D RECONSTRUCTION BY SPACE CARVING

| Resolution       | 30*30*60 | 60*60*80 | 80*80*100 |
|------------------|----------|----------|-----------|
| Number of voxels | 7656     | 18345    | 32080     |
| Time (s)         | 8        | 20       | 33        |

#### B. Evaluation :

- The quality of the 3D model obtained depends strongly on the resolution chosen.
- In contrast to the Shape From silhouette technique, we obtained a more precise and textured 3D model.
- The calculation time is longer because of the photo consistency test of each voxel.

## VI. COMPARISON

The quality of the results of different reconstruction techniques studied strongly depends on the calibration of the cameras. Therefore, the camera parameters must be well estimated.

Our comparison is based on the results of different reconstruction techniques presented in the tables: Table I, Table II, Table III, Table IV and Table V.

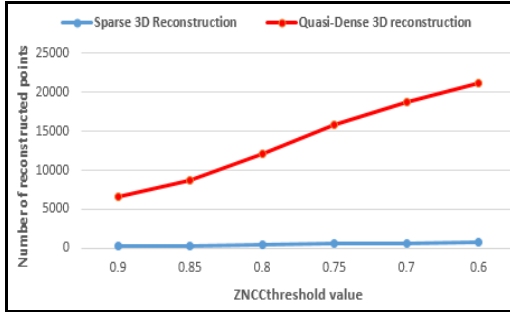


Figure 15. Number of reconstructed points as a function of the value of the ZNCCthreshold. the number of reconstructed points by quasi-dense 3D reconstruction is greater than sparse 3D reconstruction

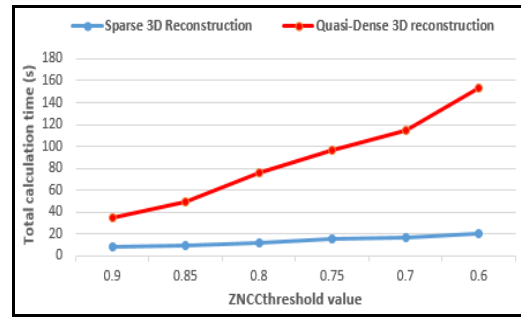


Figure 16. Total calculation time according to the value of the ZNCCthreshold. The quasi-dense 3D reconstruction requires more calculation time because of the large number of reconstructed points

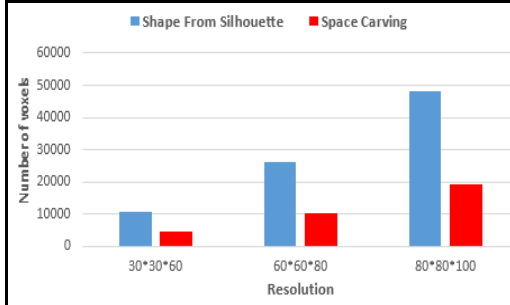


Figure 17. Total number of voxels depending on the resolution chosen. The number of voxels of reconstruction by Shape from Silhouette is greater because the model obtained is a bounding shape.

In the sparse 3D reconstruction and quasi-dense 3D reconstruction, the quality of the results depends on the quality of matching. According to the experimental results presented in Table I and Table III, for different values of ZNCCthreshold, the calculated re-projection error is included between 0.23 and 1.12. So the quality of the different results is accepted.

Shape from Silhouette technique allows the estimation of an enclosing shape (Visual hull). The quality of the result depends on the resolution chosen, the number of images used, and the quality of extraction of silhouettes. The 3D model obtained comprises a set of voxels which do not belong actually to the object. The Space Carving technique offers a solution to this problem by eliminating these remaining voxels. Moreover, it allows to get a textured 3D model.

Regarding the calculation time, the sparse 3D reconstruction is much faster than the quasi-dense 3D reconstruction, the reduced number of reconstructed points allowed to decrease the time of calculation. The Shape from Silhouette technique is also much faster than the Space Carving technique.

## VII. PROPOSED APPROACH

### A. Description

To take advantage of the methods studied. In this section, we propose an approach based on the extraction of silhouette images and the matching for a full 3D reconstruction of object from a sequence of images taken from different and suitable viewpoints (Figure 19). It consists in the matching of images

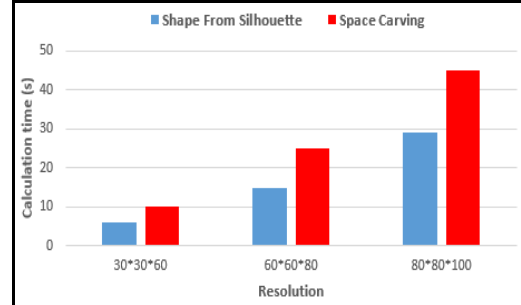


Figure 18. Calculation time according to the resolution chosen. The Space Carving technique requires more calculation time because of the photo-consistency test

points limited to the points belonging to the object silhouettes. First of all, it starts by the detection of points of interest by Harris detector (the points belonging to the object silhouette). Then, ZNCC is used for the matching of these points. To increase the density of matches and have the densest 3D reconstruction, the propagation method [11] has been used. So, instead of using the silhouette image for carving an initial 3D volume discretized into voxels, as it was presented in the Shape from Silhouette and Space carving, we use the silhouette images for limiting the search space of matches and obtain a full and textured 3D reconstruction of object. Full 3D reconstruction is achieved by fusion of the results of reconstruction between the pairs of consecutive images.

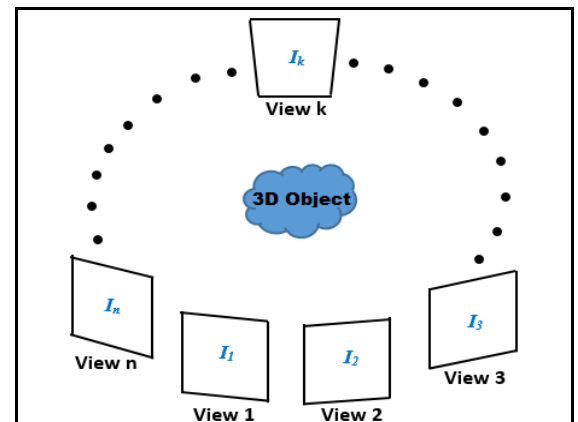


Figure 19. n images taken from different and suitable viewpoints

### **Steps :**

1. Image acquisition
2. Calibration or self-calibration
3. Silhouette extraction [13, 14]
4. Detection and matching of points of interest (the search is limited to the pixels belonging to the silhouette of the object).
5. Application of the propagation method [11] for finding new matches near the ancients (the search is always limited to the pixels belonging to the silhouette of the object).
6. Estimation of 3D points by optical triangulation
7. Fusion of the results of reconstruction between the pairs of consecutive images for a complete reconstruction of the 3D object.

### **B. Experiments**

10 images with resolution of  $640 \times 480$  pixels was used for 3D reconstruction.



Figure 20. Two images of the captured images



Figure 21. Silhouettes extraction after segmentation

After the detection of points of interest by the Harris detector, ZNCC method and the epipolar constraint were used to match these points.



Figure 22. Interest point matching

Application of the propagation method [11] for finding new matches near the ancients.



Figure 23. Matching result obtained after applying the propagation method

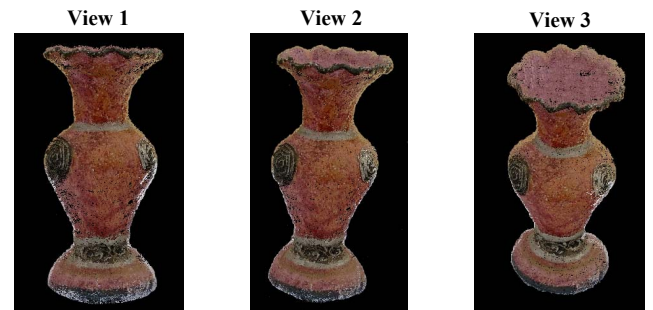


Figure 24. Different views of 3D reconstruction result

From the results obtained, the proposed method allows us to have results of quality.

### **VIII. CONCLUSION**

In this article, we made a certain kind of comparative study of the techniques of 3D reconstruction from images, that is to say passive stereo vision, Shape from Silhouette and Space Carving. For the passive stereo vision, the quality of the 3D model obtained or exactly the quality of 3D reconstructed points depends on the quality of the matches made. The calculation time relies on the number of reconstructed points. The sparse 3D reconstruction is fast, but a reconstruction after the propagation method requires more time. The Shape from Silhouette technique is a quick technique that enables the estimation of an approximate form of the object called the Visual Hull, the quality of the result depends on the quality of the extraction of silhouettes and the number of images used. The Space Carving technique allows us to have a more precise and textured 3D model. But, it requires a longer calculation time. Each technique has its strengths and weaknesses, the best solution may be to think about hybrid techniques to benefit from the advantages and avoid disadvantages of each technique. So, we proposed a method based on the use of silhouettes and matching for 3D object reconstruction from a sequence of images taken from suitable viewpoints. From the results obtained, the proposed method allows us to have results of better quality.

### **REFERENCES**

- [1] Z. Zhang. A flexible new technique for camera calibration. *IEEE Transactions on Pattern Analysis and Machine Intelligence*, 22(11):1330-1334, 2000

- [2] E. E. Hemayed "A survey of camera self-calibration", Proc. IEEE Conf. Adv. Video Signal Based Surveillance, pp.351 -357, 2003.
- [3] A.Saaidi, A.Halli, H.Tairi and K.Satori. "Self – Calibration Using a Particular Motion of Camera". In Wseas Transaction on Computer Research. Issue 5, Vol. 3, May 2008.
- [4] C.Harris and M.Stephens. A combined Corner and Edge Detector. Alvey vision Conference. pp. 147-151, 1988.
- [5] D. G. Lowe. Distinctive image features from scale-invariant keypoints. International Journal of Computer Vision, 60(2):91-110, 2004.
- [6] S.El Hazzat, A.Saaidi and K.Satori. Euclidean 3D Reconstruction of Unknown Objects from Multiple Images. Journal of Emerging Technologies in Web Intelligence, Vol. 6, No. 1, February 2014
- [7] Feipeng Da, Yihuan Sui. 3D reconstruction of human facebased on an improved seeds-growing algorithm. MachineVision and Applications, 22: 879-887, 2011.
- [8] Du Xin and Zhu Yun-fang. A flexible method for 3D reconstruction of urban building. 9th International Conference on Signal Processing, 2008
- [9] E.Vural and A. Aydin Alatan. Outlier Removal for Sparse 3D Reconstruction from Video. 3DTV Conference: The True Vision - Capture, Transmission and Display of 3D Video, 2008
- [10] M. Lhuillier and L. Quan, "Quasi-Dense Reconstruction from Image Sequence," Proc. Seventh European Conf. Computer Vision, vol. 2, pp. 125-139, Aug. 2002.
- [11] M. Lhuillier and L. Quan, "Match Propagation for Image-Based Modeling and Rendering," IEEE Trans. Pattern Analysis and Machine Intelligence, vol. 24, no. 8, pp. 1140-1146, 2002.
- [12] A. Laurentini. The visual hull concept for silhouette-based image understanding. IEEE Transactions on PatternAnalysis and Machine Intelligence, Vol.16, No.2, February 1994
- [13] W. Lee, W.Woo, and E. Boyer. Silhouette segmentation in multiple views. IEEE TPAMI, 33(7):1429-1441, july 2011.
- [14] G. Zeng and L. Quan. Silhouette extraction from multiple images of an unknown background. In Proc. of ACCV, pages 628-633, 2004.
- [15] A. Ladikos, S. Benhimane and N. Navab, "Efficient visual hull computation for real-time 3d reconstruction using cuda," in Proceedings of the 2008 Conference on Computer Vision and Pattern Recognition Workshops, 2008.
- [16] K. N. Kutulakos and S. M. Seitz. A theory of shape by space carving. International Journal of. Computer Vision, 38(3):199-218, 2000.
- [17] Anselmo Antunes Montenegro, Paulo Cesar Pinto Carvalho, Marcelo Gattass, Luiz Velho. Adaptive Space Carving. In 3DPVT, pp. 199-206, 2004.
- [18] M. A. Fischler and R. C. Bolles. Random sample consensus : a paradigm for model fitting with applications to image analysis and automated cartography. Commun. ACM, 24(6) :381-395, 1981.
- [19] D. Kim, J. Rutledge, R. Dahyot. Bayesian 3d shape from silhouettes. Digital Signal Process, 23 (6):1844-1855, 2013
- [20] Nina Amenta, Marshall Bern, and. Manolis Kamvysselis. A new Voronoi-. Based Surface Reconstruction Algorithm. SIGGRAPH '98 Proceedings, 415-421, 1998
- [21] R. Guerchouche, O. Bernier, T. Zaharia. Multiresolution volumetric 3D object reconstruction for collaborative interactions. Pattern Recognition and Image Analysis, 18:621-637, 2008.
- [22] M. Lhuillier and L. Quan. A quasi-dense approach to surface reconstruction from uncalibrated images. IEEE Transactions on Pattern Analysis and Machine Intelligence, 27(3):418-433, 2005